J Electr Eng Technol.2017; 12(1): 295-301
http://dx.doi.org/10.5370/JEET.2017.12.1.295

ISSN(Print) 1975-0102
ISSN(Online) 2093-7423

Influence Regularity of Aluminum, Copper and Stainless-steel on SF_6 PD Decomposition Characteristics Components

Fuping Zeng†, Jing Luo*, Ju Tang*, Qian Zhou and Qiang Yao****

Abstract – SF_6 decomposition products can be used to detect partial discharge (PD), but the metal materials in a PD area can significantly affect SF_6 decomposition characteristics. Disregarding the effect of metal materials on such characteristics inevitably result in certain errors when using them to diagnose the internal insulation faults of gas-insulated switchgears. This paper investigates the influence regularity on the main stable decomposition components of SF_6 (namely SO_2F_2 and SOF_2) of the commonly metal materials uesd in GIS, such as aluminum (Al), copper (Cu) and stainless steel (SS). Firstly, an experimental platform is constructed to simulate SF_6 decomposition under a PD area, and the influence regularities of Al, Cu and SS on the concentration, formation rate and saturation time of SO_2F_2 and SOF_2 are obtained. Secondly, the influence mechanism of Al, Cu and SS are preliminary explored combined with the chemical activity of the metal materials.

Keywords: GIS, Partial discharge, SF_6 decomposition, Metal materials, Influence regularity

1. Introduction

Unlike the pulse current and ultra-high frequency methods of detecting partial discharge (PD) and diagnosing insulation status, the method based on SF_6 decomposition characteristics is a highly promising method of monitoring the inner insulation faults of gas-insulated equipment, such as gas-insulated switchgear (GIS), transformer and line [1-4]. This method is also free of electromagnetic interference, and its insulation fault can be recognised qualitatively and quantitatively. PDs are generally generated from gas-insulated equipment before the occurrence of faults (e.g., insulation breakdown and flashover) caused by insulation defects [5-6]. In this case, the SF_6 insulation medium in the gas chamber decomposes and produces a series of characteristic products under the high pulsed electromagnetic energy of PDs. The content and variation regularity of these characteristic components can effectively represent the PD pattern, severity and developing tendency of the insulation fault [7-8]. The International Council on Large Electric Systems has established the WGB3-25 work group, which is designed to formulate guidelines for the SF_6 analysis of the diagnosis of the insulation faults of GIS or other SF_6-insulated equipment.

However, the SF_6 decomposition characteristics under PD are not only related to the insulation fault pattern and PD energy but are also closely associated with the type of metal electrode material in the PD location [9,10]. The metal material in the discharge area can react with primary decomposed products (low fluoride SF_x) and react into metal fluorides [11,12]. Nevertheless, given that SF_x is the key factor in the formation of the final decomposed products of SF_6, such as SO_2F_2 and SOF_2, the difference in the metal electrode material can significantly affect the SF_6 decomposition characteristics. If the difference in the metal electrode material is disregarded and the information of the decomposed component is directly exploited to diagnose the SF_6 electrical equipment, an assessment deviation is inevitably produced; misjudgement may even arise in serious conditions. Hence, studying the influence regularity of different metal electrode materials on SF_6 decomposition characteristics is important. Clarifying whether or not the main stable components can be used to recognise metal materials in a PD area and determining whether or not the influence of metal electrode materials can be amended at comparable levels are also crucial. All these factors can provide a reliable basis for correcting the major deviation caused by the difference in the metal electrode materials.

Few researchers, such as A. M. Casanoas, R. Kurte and C. Beyer, have investigated the influence regularity of different metal electrode materials on SF_6 decomposition characteristics[9,13,14]. These researchers mainly investigated the SF_6 decomposition characteristics of typical metal materials, such as Al, Cu and SS. Their results show that the SF_6 decomposition characteristics of different metal electrode materials have obvious discrepancies. However, researchers have not yet investigated further whether or not the type of metal electrode material in the PD location can be recognised using the main stable component. Researchers are also yet to develop a correction method of amending the discrepancy of various

† Corresponding Author: School of Electrical Engineering, Wuhan University, China. (Fuping.Zeng@whu.edu.cn)
* School Electrical Engineering, Wuhan University, China. (295259620@qq.com, cqtangju@whu.edu.cn)
** State Grid Chongqing Electric Power Company, China. (cquzhou@163.com, yaoqiang212@aliyun.com)
Received: August 13, 2015; Accepted: October 22, 2016

metal electrode materials.

Given this context, the present study establishes the needle-plate fault model of three typical metal electrode materials (Al, Cu and SS) and clarifies the influence regularity of metal electrode materials on the content, formation rate and saturation trend of the characteristic components and the component concentration' ratio $C(SO_2F_2)/C(SOF_2)$. The correlation coefficients of the decomposition characteristics of Al, Cu and SS are calculated, and the discriminating factor that rectifies the influence of these metal materials is proposed based on the single component $C(SO_2F_2)$, $C(SOF_2)$ and feature decomposition sum $C(SO_2F_2, + SOF_2)$.

2. Experimental

2.1 The SF_6 decomposition System

Fig. 1 shows the designed SF_6 decomposition gas chamber [15], The volum of experimental chamber was 60L. This study used the needle-plate electrode model to simulate the most common metal protrusion faults of the SF_6 electrical equipment and to obtain the SF_6 decomposition characteristics under the PDs of the three metal materials. A stable PD was produced by applying the testing voltage on the needle electrode through high-voltage bushing. This was used to simulate a discharge situation in

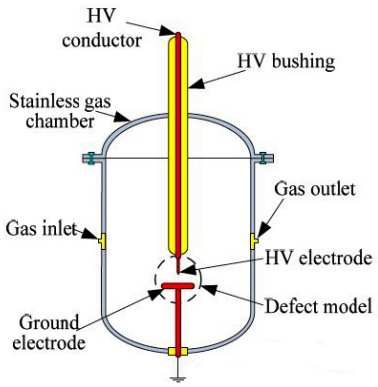

Fig. 1 SF_6 decomposition chamber under PD

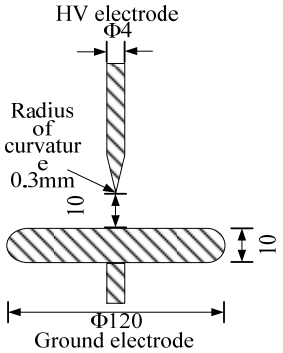

Fig. 2 The Electrode structure (unit: *mm*)

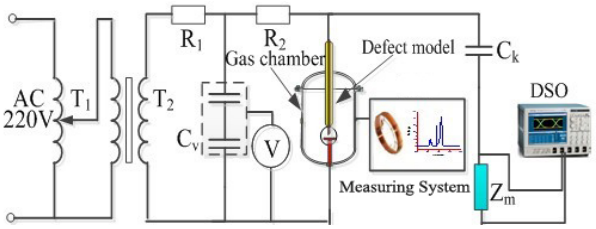

Fig. 3 Test wiring diagram

the actual gas chamber of the SF_6-insulated equipment. The gas pressure in the gas chamber was 0.4 MPa, the SF6 purity was 99.995%, and the distance between the needle and the plate was 10 mm. The most typical metal materials in the SF_6-insulated equipment were selected for the fault model: aluminum (Al), copper (Cu) and 304 stainless steel (06Cr19Ni10, SS). In order to reduce the error caused by the structure size of the electrode to the experimental results, all the electrode structure in the experiment were the same, and the process was in accordance with the grade of tolerance of IT0 . The structure size is shown in Fig. 2.

The testing wiring diagram of the system is shown in Fig. 3. A voltage regulator (T_1: 0 V to 380 V) and testing transformer (T_2: 10 kVA/50 kV) comprised the ac-testing supply. A protective resistance (R_1, R_2: 10 kΩ) was used to protect the transformer and the system. A capacitive voltage divider (Cv) was used to measure the testing voltage value. Given that it can provide a high-frequency low-resistance pathway to extract the pulse voltage, C_k (2023 pF/100 kV) was used as the coupling capacitance. A non-inductive detection impedance (Zm: 50 Ω) was used to send the pulse current signal to the oscilloscope. A digital storage oscilloscope (WavePro 7100XL, analogue band: 1 GHz; sampling rate: 20 GHz; memory depth: 48 MB) was used to monitor the real-time PD magnitude and quantitatively calibrate the PD.

A gas chromatograph (GC: Varian CP-3800) was used in the experiment to quantitatively measure the sample gas components produced by the discharge. A packed column Porapak QS and a special capillary column CP-Sil5CB were used in parallel in the GC to separate the components in the mixture. Double pulsed discharge helium ionisation detectors, with a detection precision of up to 0.01 ppm, were also used to quantitatively detect each separated component. The working conditions were as follows: the carrier gas was He (purity: 99.9995%); the flow rate was 2 mL/min; the constant column temperature was 40 °C; the sample size was 1 mL; and the split ratio was 10:1. This GC can effectively measure components, such as SOF_2, SO_2F_2, CF_4 and CO_2, and can produce highly accurate and stable measurements.

2.2 Testing method

To reduce the influence of the ambient environment on the resting result, all the experiments in this study were

conducted at a temperature of 20 ± 3 °C and a humidity of 50% ± 5%; the H_2O content was also controlled to less than 50 ppm. The specific steps are as follows:

2.2.1 Cleaning the gas chamber.

The needle-plate insulation fault model was placed in a gas chamber. The gas chamber was then vacuumed (0.002 MPa), filled with new gas (SF_6) and then vacuumed again. This process was repeated thrice for purification and to prevent the remaining impurities from affecting the testing results.

2.2.2 Filling in the new SF_6.

After cleaning, the gas chamber was filled with 0.4 MPa of the new SF_6. The H_2O and O_2 contents were measured using a dew-point instrument DMP-10 and an HF-YF oxygen analyser. The H_2O and O_2 contents in the gas chamber were then checked to ensure that they satisfy the industrial standard DL/T596-1996 requirements. The next step was taken, or Step (1) was repeated.

2.2.3 Applying the testing voltage.

The electrical wiring of the system was connected, as shown in Fig. 3. The experimental voltage was gradually increased to the required voltage, and the discharge magnitude was monitored. Without utilising the insulation fault model, the PD inception voltage of the equipment (U_s) was 45 kV. After employing the needle-plate fault model, the PD inception voltage (U_0) of the equipment was 23 kV. The final experimental voltage was 37.5 kV. The needle-plate fault model was applied in each metal electrode material at the same voltage.

We used the pulse current method to calibrate and monitor the discharge magnitude, as recommend in IEC 60270. Because of the randomness and complexity of PD process itself, in order to comprehensively monitor the PD characteristics of different metal materials, 150 discharge sample data were randomly collected before the sample gas was collected. The colleting times were a total of 8 times, including a total of 1200 sample data, and then the sample data was statistically analysed.

The statistical characteristics of PD quantity of different metal materials under needle plate electrode with the 37.5kV test voltage is shown in Fig. 4. The discharge amount of PD under needle plate electrode with different metal materials was different, but the discharge quantity was close to the normal distribution, as shown in Fig. 4. Therefore, with the statistical average value calculated, the statistical average value can be used as a description of the PD discharge quantity under needle plate electrode with each metal materials .The statistical average value is shown in Table 1. Under the applied testing voltage, Table 1 shows the average discharge quantity of the different metal electrode materials. According to the details

Table 1 Average discharge magnitude of the PD

Metal electrode	Al	Cu	SS
Discharge magnitude/pC	80.1	75.6	78.4

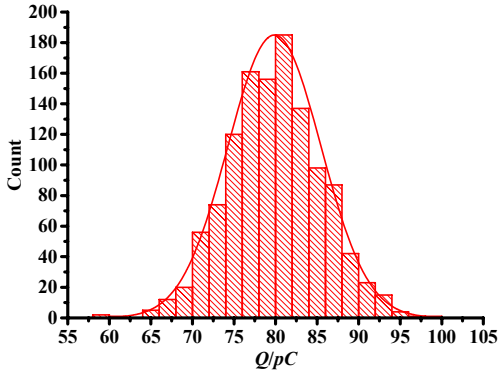

(a) Al

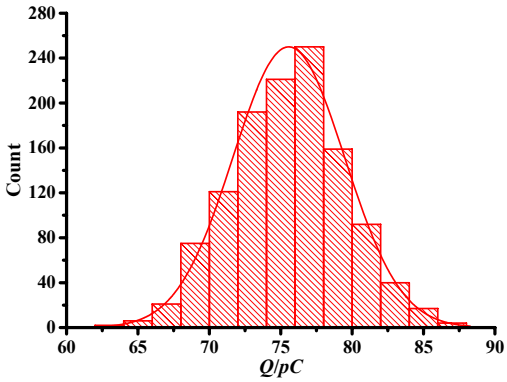

(b) Cu

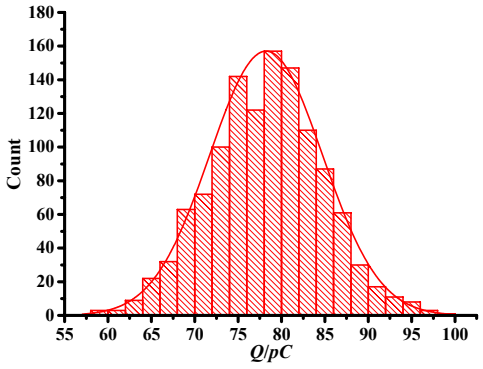

(c) SS

Fig. 4 The statistical properties of PD discharge quantity under needle plate electrode of different metal materials

displayed on this table, the average discharge quantities of the different metal electrode materials are almost the same. Hence, the difference in PD quantity cannot possibly lead to the discrepancy of the SF_6 decomposition characteristics.

2.2.4 Measuring the decomposed component.

The decomposition experiment on each electrode metal

material under PD was conducted for 96 h. A specific sampling bag was used to collect the sample gas from the outlet every 12 h. A GC was used to quantitatively analyse the decomposed components and obtain the decomposition characteristics of the three metal electrode materials.

(5)Concluding the experiment. After measurement, the gas chamber was vacuumed and was left for 24 h. This step was performed to reduce the influence of the used gas chamber on the following experiment. Step (1) was then repeated to prepare the gas chamber for another experiment.

3. Influence Regularity of Metal Electrode Materials on SO_2F_2 and SOF_2

Based on the "zone model of SF_6 decomposition mechanism" provided by R. J. Van Brunt [16] and other related investigations [10-12], the main gas components of SF_6 decomposition under PD include HF, CF_4, CO_2, SO_2F_2, SOF_4 and SOF_2, where HF is a strong acidic substance which can easily react with metals and insulation materials, thereby decreasing the amount of HF as the discharge time increases. SOF_4 can easily hydrolyse and is unstable; CF_4 and CO_2 are mainly used to reflect the degradation status of solid organic insulation materials, which are not discussed in the present study. In contrast to these components, SO_2F_2 and SOF_2 are the more obvious and stable factors of SF_6 decomposition under PD. They can also effectively reflect the deterioration degree of the SF_6 insulation property and the strength of the PD energy [7,17]. Hence, SO_2F_2 and SOF_2 are selected as the most characteristic components to represent the influence regularity of different metal electrode materials on SF_6 decomposition characteristics under PD.

Given the complexity of the decomposition process, the experimental data are obtained as three-time experiments under the same ambient condition, the SO_2F_2, SOF_2 and $SO_2F_2+SOF_2$ concentrations with different electrode materials are obtained after 96 h, as shown in Figs. 5~6 respectively. In addition, to describe the experimental results more objective, the error bar has been given in Figs. 5~7. Metal electrode materials exert apparent effects on SO_2F_2 and SOF_2 formations. In terms of concentration value, the SO_2F_2 of Al is higher than that of Cu, and the SO_2F_2 of Cu is higher than that of SS. Moreover, each SO_2F_2 at different electrode materials can enter a saturation status after some discharge time, but the saturation points of these electrode materials differ. The saturation time of Al is the shortest, followed by Cu and SS. However, the SOF_2 formation rate under the PDs of the three metal electrodes remains stable, as shown in Fig. 6. Each of the metal electrodes presents a linear growth trend during the experimental period. Among these metal electrodes, the SOF_2 under the Al electrode has the most significant tendency to increase, followed by the SOF_2 under the Cu electrode and the SOF_2 under the SS electrode.

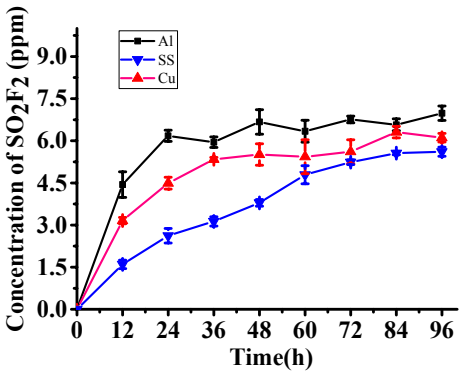

Fig. 5 Variation regularity of the SO_2F_2 amount with time

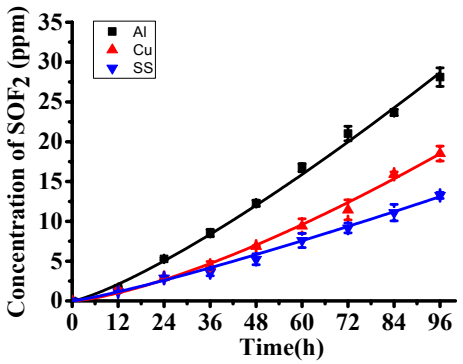

Fig. 6 Variation regularity of the SOF_2 amount with time

The main reason behind this finding is that the metal electrode material under PD engages in an SF_6 decomposition reaction at the surface area where the solid metal material is in contact with the gaseous SF_6. Therefore, the elementary decomposed products SF_x and F atoms with extremely high reactivity are generated. When these substances diffuse into the material surface of the metal electrodes, they further react with the metals and produce low fluorine sulphur and metal fluorides.

$$nSF_6 + 2M \rightarrow nSF_4 + 2MF_n \quad (1)$$

$$nSF_5 + M \rightarrow nSF_4 + MF_n \quad (2)$$

$$nSF_6 + 4M \rightarrow nSF_2 + 4MF_n \quad (3)$$

$$2nSF_6 + 10M \rightarrow nS_2F_2 + 10MF_n \quad (4)$$

$$M+nF^* \rightarrow MF_n \quad (5)$$

These low fluorine sulphurs (e.g., SF_4 and SF_2) diffuse into the main chamber and can react with trace H_2O and O_2 that are mixed in the SF_6, thereby producing the characteristic components SOF_2 and SO_2F_2, as shown in the following:

$$SF_2 + O_2 \rightarrow SO_2F_2 \quad (6)$$

$$SF_4 + H_2O \rightarrow SOF_2 + 2HF \quad (7)$$

Hence, the participation of metal materials in SF_6

decomposition under PD breaks the decomposition–recombination balance of SF_6. In this case, metal materials can promote the SF_6 decomposition process, and the formation of the decomposed component characteristics can be positively affected.

During the experiment, the chemical reaction between the metal materials and the elementary decomposed product SF_x is mainly located at the glowing area around the electrode surface. The chemical reaction rate can be affected by factors, such as reactant property, reactant granular size, reaction contact area, temperature and pressure. The ambient condition of the experiment is maintained. In this case, the influence of electrode materials on SF_6 decomposition is mainly subject to the chemical activity of the electrode metal. Therefore, the chemical activity of the metal is the most important factor in reaction speed, as shown in Reactions (1) to (5). The metal with the high activity can contribute to a large reaction rate with SF_6, thereby generating more decomposed components.

In the experiment, SAE 304 stainless steel is adopted as the stainless steel electrode material; it contains 74% iron, 18% chrome and 8% nickel. Given that this material contains large amounts of chrome and nickel, an austenite structure can be formed. As a result, metal passivation occurs, and the chemical activity of stainless steel is reduced significantly. Among the three metal materials, Al has the highest chemical activity, followed by Cu and then SS. The higher the chemical activity of the metal is, the quicker the reaction rate, and the higher the amount of the decomposed by-products. In this case, the decomposition rate of SF_6 under the Al electrode is the highest among all the electrodes. Given the low PD quantities during the experiment, the amounts of SO_2F_2 under the three metal electrodes are all small. In addition, all the SO_2F_2 under the three metals increases and presents a saturation trend with the discharge time, where the saturation concentration of all the SO_2F_2 are almost similar. However, the saturation time of the SO_2F_2 distinctly differs; the time SO_2F_2 takes to saturate under the Al electrode is the shortest, whereas that under the SS electrode is the longest, as shown in Fig.5.

On one hand, the generated metal fluorine is in the solid state, and most of them directly attach to the electrode surface and form a dense layer, which reduces the reaction rate and prohibits any further generation of products. On the other hand, SF_2 can react with O_2 and produce SO_2F_2, and SF_4 can react with H_2O and produce SOF_2. In this case, the SO_2F_2 and SOF_2 formations are closely related to the O_2 and H_2O contents in the gas chamber. During the experiment, the H_2O and O_2 contents in the gas chamber are limited; the IEC 60376 and Industry Standard DL/T/596/1996 of China state that the H_2O content in the main chamber should be below 500 ppm and the air content should be below 1%. The H_2O content in the SF_6 during the actual experiment is less than 50 ppm, and the O_2 content is less than 15 ppm. When the H_2O and O_2 contents are somehow consumed, the SO_2F_2 generation rate decreases and approaches zero, which means that the SO_2F_2 formation tends to saturate.

Generating SO_2F_2 mainly depends on the O_2 and SF_2 contents. During the experiments on the three metal electrodes, the O_2 content in the gas chamber is quite low and varies slightly. As such, when the O_2 is somehow consumed, all the SO_2F_2 amounts under the three metal electrodes enter saturation. The SO_2F_2 concentrations during saturation do not differ largely from one another.

The chemical activity of metal materials is also important in the reaction rate between the metal and the elementary decomposed component SF_x. Metals with stronger activities therefore react more violently with SF_x, produce more SF_2, thereby eventually forming more SO_2F_2, than metals with weak activities. However, given the limited O_2 content, O_2 can be consumed quickly with a high activity metal, thereby resulting in the early saturation of the SO_2F_2. Consequently, the SO_2F_2 under the Al electrode enters saturation first, followed by that under the Cu electrode and then that under the SS electrode (Fig. 5).

However, when SF_4 and H_2O undergo a hydrolysis reaction (7), and produce both SOF_2 and HF. HF can react with metal oxides at the electrode surface and produce H_2O again. In this case, a new condition (H_2O) can be provided to produce SOF_2. Hence, during the whole experiment, the SOF_2 maintains an increasing trend and presents no saturation status as in the case of SO_2F_2 (Fig. 6).

If the variation regularity of only a single component under different electrode metal materials is considered, revealing the overall degradation status of SF_6 is difficult. Given that SO_2F_2 and SOF_2 are the most significant and characteristic components of SF_6 decomposition under PD, the sum of SO_2F_2 and SOF_2 can somehow reflect the overall degradation status of SF_6. Hence, we define the sum of SO_2F_2 and SOF_2 as the feature decomposition sum ($C(SOF_2 + SO_2F_2)$) to represent the overall degradation status of SF_6. The influence of different metal electrode materials on the overall degradation of SF_6 under PD is investigated in this manner.

Fig. 7 shows the variation regularity of the feature decomposition sum under three metal electrode materials. The figure illustrates that both the amount and formation

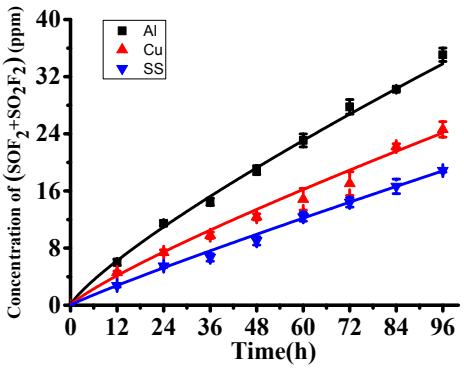

Fig. 7 Feature decomposition sum $C(SO_2F_2 + SOF_2)$

rate of the feature decomposition sum present apparent differences under each material. Al has the highest difference, followed by Cu, and then SS. This difference reveals that $C(SOF_2 + SO_2F_2)$ can well recognise the influence of different metal electrode materials. In addition, the curves of Al, Cu and SS have similar increasing trends with time development. Therefore, certain relationships exist among the influences of the different metal electrode materials on $C(SOF_2 + SO_2F_2)$.

4. Conclusion

(1) The chemical activity of metal material can directly affect the decomposition process of SF_6 under PD. Metal electrode material has greatly affects on the generation rate of SO_2F_2 and SOF_2. It is because the formation rate of low fluorine sulphurs and fluorine atoms produced by SF_6 decomposition increases with the improvement of chemical activity of metallic electrode material. The metallic electrode material with higher chemical activity will have more obvious promotion impact and produce more SF_2 and SF_4, which will further react into more SOF_2 and SO_2F_2. That is to say, the relationship of the concentration and formation rate of these metal electrode materials are as follows: Al > Cu > SS. In other word, when use SF_6 decomposition characteristics to diagnosis and assess the insulation fault of GIS, the influence of metal materials should be considered.

(2) Because of the metal electrode materials (Al, Cu and SS) play key roles on the formation of characteristic decomposed components of SF_6 during PD and have significant influence on the products, so it is necessary to further study the influence mechanism of metal electrode materials under PD, which will help achieve sufficient knowledge on what influences the regularity in the reactions to propose correction methods accordingly. Acquiring sufficient knowledge on the decomposition mechanism and the factors that affect variation in the reactions under PD will lay a solid foundation in using decomposed components of SF_6 to assess insulation status and will support related repair guidelines for gas insulated electrical equipment.

Acknowledgements

This research was funded by the National Natural Science Foundation of China (Grant No. 51607127), Special Project of China Postdoctoral Science Foundation (Grant No. 2016T90723), China Postdoctoral Science Foundation (Grant No.2015M582271) and Natural Science Foundation of Hubei Province (2015CFB165). Express sincerely thankfulness here.

References

[1] Judd M D, Farish O, Hampton B F. "The excitation of UHF signals by partial discharges in GIS," IEEE Transactions on Dielectrics and Electrical Insulation, vol. 3, pp. 213-228, 1996.

[2] IEC 60270 High-voltage test techniques-partial discharge measurement, 2000.

[3] F. Y. Chu, "SF_6 Decomposition in Gas-Insulated Equipement," IEEE Transactions on Electrical Insulation, vol. EI-21, p. 33, 1986.

[4] L. G Christophorou, J. K. Olthoff and R. J. Van Brunt, "Sulfur Hexafluoride and the Electric Power Industry," IEEE Electrical Insulation Magazine, vol. 13, pp. 20-24, 1997.

[5] Heise H M, Kurte R, Fischer P, et al. "Gas analysis by infrared spectroscopy as a tool for electrical fault diagnostics in SF_6 insulated equipment," Fresenius' Journal of Analytical Chemistry, vol. 358, pp. 793-799, 1997.

[6] Ding W, Hayashi R, Ochi K, et al. "Analysis of PD-generated SF_6 decomposition gases adsorbed on carbon nanotubes," IEEE Transactions on Dielectrics and Electrical Insulation, vol. 13, pp. 1200-1207, 2006.

[7] Ju Tang, Fuping Zeng, Jianyu Pan, et al. "Correlation Analysis Between Formation Process of SF_6 Decomposed Components and Partial Discharge Qualities," IEEE Transactions on Dielectrics and Electrical Insulation, vol. 20, pp. 864-875, 2013.

[8] Luo Lishi, Yao Wenjun, Wang Jun, et al. "Research on partial discharge diagnosis of GIS by Decomposed Gas of SF_6," Power System Technology, vol. 34, pp. 225-230, 2010.

[9] Casanovas A M, Casanovas J, Lagarde F, et al. "Study of the decomposition of SF_6 under dc negative polarity corona discharges (point to plane geometry): Influence of the metal constituting the plane electrode," Journal of applied physics, vol. 72, pp. 3344-3354, 1992.

[10] Tang J, Liu F, Zhang X, et al. "Partial discharge recognition through an analysis of SF_6 decomposition products part 1: decomposition characteristics of SF_6 under four different partial discharges," IEEE Transactions on Dielectrics and Electrical Insulation, vol. 19, pp. 29-36, 2012.

[11] MacGregor S J, Woolsey G A, Ogle D B, et al. "The influence of electrode-fluorine reactions on corona and glow discharges in SF_6, " IEEE Transactions on Plasma Science, vol. 14, pp. 538-543, 1986.

[12] Van Brunt R J, Herron J T. "Fundamental processes of SF_6 decomposition and oxidation in glow and corona discharges," IEEE Transactions on Electrical Insulation, vol. 25, pp. 75-94, 1990.

[13] Beyer C, Jenett H, Klockow D. "Influence of reactive SF_6 gases on electrode surfaces after electrical dis-

charges under SF_6 atmosphere," IEEE Transactions on Dielectrics and Electrical Insulation, vol. 7, pp. 234-240, 2000.
[14] Kurte R, Beyer C, Heise H, et al. "Application of infrared spectroscopy to monitoring gas insulated high-voltage equipment: electrode material-dependent SF_6 decomposition," Analytical and Bioanalytical Chemistry, vol. 373, pp. 639-646, 2002.
[15] Tang Ju, Li Tao, Wan Lingyun, et al. "Device of SF_6 dissociation apparatus under partial diacharage and gaseous decomposition components analysis system," High Voltage Engineering, vol. 34, pp. 1583-1588, 2008.
[16] Van Brunt, R. J., and J. T. Herron. "Plasma chemical model for decomposition of SF_6 in a negative glow corona discharge," Physica Scripta, vol. T53, pp. 9-29, 1994.
[17] Tang J, Liu F, Zhang X, et al. "Characteristics of the Concentration Ratio of SO_2F_2 to SOF_2 as the decomomposition products of SF_6 under corona discharge," IEEE Transactions on Plasma Science, vol. 40, pp. 56-62, 2012.

Fuping Zeng was born in Chongqing, China in 1984. He obtained his bachelor's degree in electrical engineering from Dalian Maritime University, and his master's and doctoral degrees from the State Key Laboratory of Power Transmission Equipment & System Security and New Technology, Chongqing University, China. He is currently a post-doctoral research at the School of Electrical Engineering, Wuhan University, China. He is involved in the online monitoring and fault diagnosis of high-voltage electric equipment insulation.

Jing Luo She was born in Zigong, Si Chuan Province, China in 1992. She obtained her bachelor's degree from Qingdao Technological University, and she pursued a master's degree in Wuhan University since 2015.

Ju Tang was born in Pengxi, Si Chuan Province, China in 1960. He obtained his bachelor's degree from Xi'an Jiaotong University, and his master's and doctoral degrees from Chongqing University. Dr. Tang is a professor at the State Key Laboratory of Power Transmission Equipment and System Security and New Technology, Chongqing University; a professor at the School of Electrical Engineering in Wuhan University, China; and the chief scientist presiding over the National Basic Research Program of China (973 Program) (2009CB724500). He is currently involved in the online monitoring and fault diagnosis of high-voltage electric equipment insulation.

Qian Zhou was born in Kaifeng, Henan Province, China, in 1980. She received the Bachel/Master and doctoral degrees in electrical engineering from Chongqing University, China. She is now working in State Grid Chongqing Electric Power Company, China, and she is involved in on-line high voltage detection equipment and signal processing .

Qiang Yao was born in Chongqing, China, in 1971. He received the Bachelor's and Master's degrees at Chongqing University. Currently, he is a senior engineer in the Chongqing Power Company, and engaged in the analysis of the decomposition components of SF_6.